Arabian Journal of Chemistry (2015) xxx, xxx–xxx

King Saud University

Arabian Journal of Chemistry

www.ksu.edu.sa
www.sciencedirect.com

ORIGINAL ARTICLE

Comprehensive study on L-Proline Lithium Chloride Monohydrate single crystal: A semi organic material for nonlinear optical applications

Kanika Thukral [a,b], N. Vijayan [b,*], Sonia [a,b], D. Haranath [b], K.K. Maurya [b], J. Philip [c], V. Jayaramakrishnan [d]

[a] *Academy of Scientific and Innovative Research, CSIR-National Physical Laboratory, New Delhi 110 012, India*
[b] *CSIR-National Physical Laboratory, Dr. K.S. Krishnan Road, New Delhi 110 012, India*
[c] *Department of Basic Sciences, Amal Jyothi College of Engineering, Kanjirappally, Kottayam 686518, Kerala, India*
[d] *Centro De Investigations En Optica, Loma del Bosque 115, Colonia Lomas del Campestre, León, Guanajuato 37150, Mexico*

Received 19 June 2015; accepted 14 August 2015

KEYWORDS

X-ray diffraction;
Crystal growth;
Photoluminescence;
Thermal conductivity;
Specific heats;
Thermal diffusivity

Abstract L-Proline Lithium Chloride Monohydrate single crystal has been successfully synthesized and grown by slow evaporation solution technique. The lattice dimensions have been calculated by single crystal XRD. The presence of strain inside the crystal has been evaluated by powder X-ray diffraction. Its crystalline perfection was found to be good with the full width at half maxima of 29.31 arc sec. The crystal quality can be further examined by time resolve photoluminescence spectroscopy. The dielectric constant and dielectric loss have been measured over the frequency range of 10 Hz–10 kHz. The curve plotted during the measurement suggests that the value of dielectric constant decreases at higher frequency which ensures that the crystal is good candidate for NLO devices. The laser damage threshold measurements have been performed for single and multiple shots which reveal that the tolerance power for the single shot is more as compared to multiple shots. Its third order nonlinearity and thermal parameters have also been assessed for the title compound. The interference patterns obtained from the birefringence studies infer the optical homo-

* Corresponding author at: Crystal Growth and X-ray Analysis Section, CSIR-National Physical Laboratory, Dr. K.S. Krishnan Road, New Delhi 110012, India. Tel.: +91 11 45608263; fax: +91 11 45609310.
E-mail addresses: nvijayan@nplindia.org, vjnphy@yahoo.com (N. Vijayan).

Peer review under responsibility of King Saud University.

Production and hosting by Elsevier

http://dx.doi.org/10.1016/j.arabjc.2015.08.022

Please cite this article in press as: Thukral, K. et al., Comprehensive study on L-Proline Lithium Chloride Monohydrate single crystal: A semiorganic material for non linear optical applications. Arabian Journal of Chemistry (2015), http://dx.doi.org/10.1016/j.arabjc.2015.08.022

geneity and defects in the grown crystals. The density of the single crystal has been calculated by floating technique taking kerosene as a reference.

1. Introduction

In the present technological era, there is a huge demand for efficient nonlinear optical devices to fulfill the day to day requirement. Usually amino acids have asymmetrical structure which shows excellent NLO characteristics. Due to this reason it becomes essential to grow more and more new amino acid based single crystal. From the past few decades most of the scientists emphasize their work on organic materials as it show high nonlinear coefficient in comparison with inorganic. But apart of their nonlinearity, in most of the organic compounds, the molecules are attached with weak van der Walls and hydrogen bonds which make the compound soft (Kalaiselvi et al., 2008; Krishnan et al., 2013; Kushwaha et al., 2010; Suresh Kumar et al., 2006; Chemla and Zyss, 1987). On the other hand the inorganic materials are highly stable and hard but they didn't possess NLO behavior. In this context it becomes necessary to investigate the new series of semiorganic material which carries the symptoms of both organic and inorganic materials.

Proline is an abundantly available amino acid which is rigid and directional in biological system, as its amine group is part of pyrrolidine ring which is an exception from other amino acids. L-Proline cadmium chloride monohydrate, L-Proline Zinc chloride, L-Prolinium picrate, L-Prolinium Phosphite, L-Prolinium Tartrate are the series of L-proline based organic and semiorganic (Thukral et al., 2014a; Balamurugaraj et al., 2013; Uma Devi et al., 2008; Fleck et al., 2015; Chemla and Zyss, 1987; Thukral et al., 2014b) compounds which show excellent SHG efficiency. In this category, L-Proline Lithium Chloride Monohydrate is a new type of nonlinear optical material whose single crystal shows 60% transmittance which supports Second Harmonic Generation (SHG) efficiency. The SHG efficiency of the title compound is 0.2 times of KDP, which has already been reported (Uma Devi et al., 2009).

In the present report, we have carried out systematic analyses on High Resolution X-ray Diffraction (HRXRD) and Photoluminescence (PL) techniques. The optical, electrical, thermal and its third order nonlinearity properties have also been carried out in order to know its suitability for device fabrication. To the best of our knowledge this is the first report which carries structural, optical and electrical information about the title compound.

2. Growth of L-Proline Lithium Chloride Monohydrate (LPLCM) single crystal

In the present experimental study, we have adopted the slow evaporation solution growth technique. Initially, the commercially available raw materials of L-Proline and Lithium Chloride Monohydrate (LPLCM) were taken in the equimolar ratio for synthesis. These raw materials were further set to recrystallization for getting the desired compound. Once the desired compound was formed, the salt was then mixed in a double distilled water to make a saturated aqueous solution. This aqueous solution was further filtered using Whatmann filter paper to remove all the impurities and dust particles. The temperature fluctuation can be avoided by keeping the purified solution in constant temperature bath for 25 days at 35 °C. After 25 days, completely optical transparent single crystal has been harvested from the mother solution of dimension $20 \times 4 \times 3\ mm^3$ which is shown in Fig. 1.

3. Characterization

3.1. Single crystal and Powder X-ray diffraction (XRD)

The grown L-Proline Lithium Chloride Monohydrate (LPLCM) single crystal is subjected to single crystal XRD by using Bruker APEX CCD diffractometer. The source used in this analysis is graphite monochromated Mo Kα radiation ($\lambda = 0.71073$ Å). The study reveals that the LPLCM single crystal belongs to monoclinic crystal system having lattice dimensions of $a = 7.7641$, $b = 5.3757$, $c = 10.3254$ with the space group of $P2_1$ which shows a suitable concurrence with the reported literature (Uma Devi et al., 2009). The space group indicates that the crystal is a noncentrosymmetric which is an elementary condition for SHG applications.

The diffracted planes present inside the crystal can be depicted out along the different angles (i.e. 2θ) by using powder X-ray diffraction. The single crystal was crushed into fine powder and then subjected to Rigaku X-ray diffractometer with Cu Kα radiation ($\lambda \sim 1.54$ Å) with scan speed of 4°/min over a range of 20–70°. The diffraction pattern was obtained along the 2θ values which are shown in Fig. 2(a). The strain calculations can be performed with respect to the data obtained from powder XRD by using Hall Williamson equation $\beta \mathrm{Cos}\theta = K\lambda/\tau + \eta \sin\theta$, where β, θ, K, λ and τ are full width at half maxima (FWHM) of diffraction peak, Bragg diffraction angle of the peak, Scherrer constant, wavelength of X-rays and crystallite size respectively. The value of the strain was measured with the slope drawn against the curve of $\beta \mathrm{Cos}\theta$ Vs $\mathrm{Sin}\theta$ shown in Fig. 2(b). The slope value (η) is

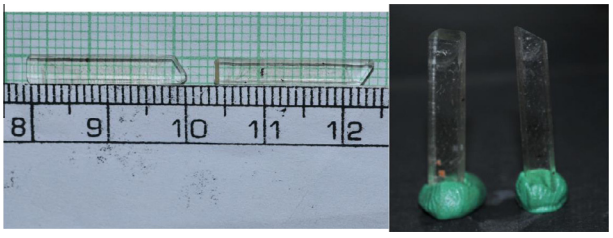

Figure 1 Harvested L-Proline Lithium Chloride Monohydrate single crystal from mother solution.

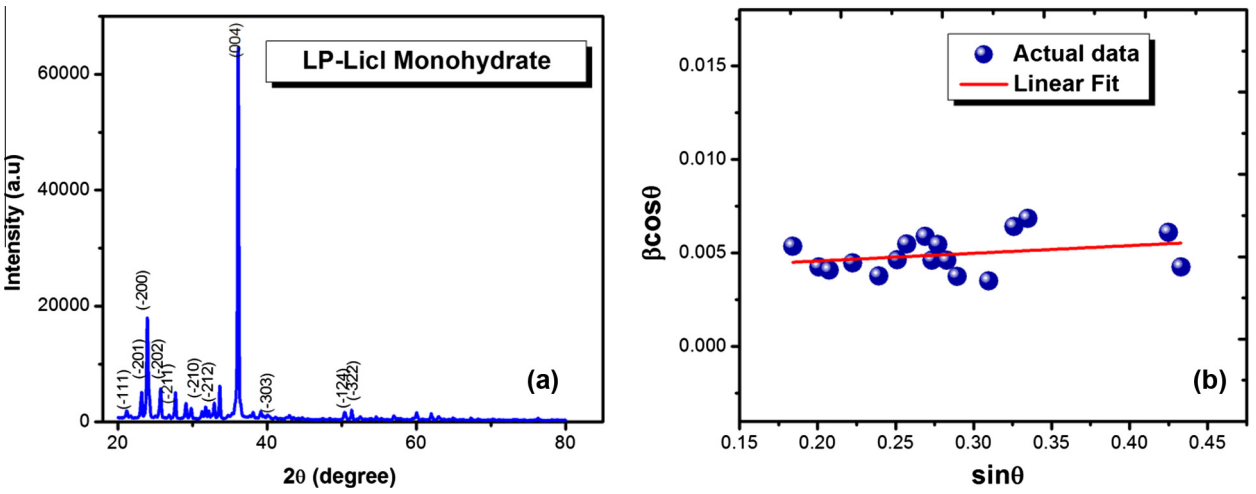

Figure 2 Powder X-ray diffraction pattern along with $\beta \mathrm{Cos}\,\theta$ versus $\sin\theta$ plot.

0.004 with slight error of 0.00353 which suggests that the crystal carries compressive strain.

3.2. Crystalline perfection

A PANalytical X'Pert PRO MRD high-resolution XRD system, with Cu $K\alpha_1$ radiation, was employed to assess the crystalline perfection of the grown crystal. The rocking curves of the crystal for the diffraction planes were recorded in symmetrical Bragg geometry using the natural facets by performing the ω scan (Bhagavannarayana et al., 2010) with double-axis geometry. The monochromated X-ray beam incident on the specimen was obtained using a high-resolution four-bounce Ge(220) monochromator. The diffracted beam from the specimen was detected using a scintillation detector without using any analyzer at the receiving stage (i.e. before the detector) to get all the possible information such as the individual peaks from structural grain boundaries, scattered intensity from the dislocations and other defects from the specimen crystal.

Fig. 3 shows the high-resolution diffraction curve (DC) recorded for a typical LPLCM single crystal specimen using (−2 1 1) diffracting planes in symmetrical Bragg geometry with Cu $K\alpha_1$ radiation. As seen in the figure, the DC contains a single peak and indicates that the specimen is free from structural grain boundaries. The full width at half maximum (FWHM) of this curve is 29 arc sec which is somewhat more than that expected from the plane wave theory of dynamical X-ray diffraction (Batterman and Cole, 1964) and reveals the presence of point defects and their aggregates. It is interesting to see the shape of the DC. The DC is asymmetric with respect to the Bragg peak position. For a particular angular deviation ($\Delta\theta$) of glancing angle (θ) with respect to the Bragg peak position (taken as zero for the sake of convenience), the scattered intensity is much more in the negative direction in comparison with that of the positive direction. This feature clearly indicates that the crystal contains predominantly vacancy type of defects than that of interstitial defects. This can be well understood by the fact that due to vacancy defects, the lattice around these defects undergoes tensile stress (Bhagavannarayana et al., 2008) and the lattice parameter d (interplanar spacing) increases and leads to give more scattered (also known as

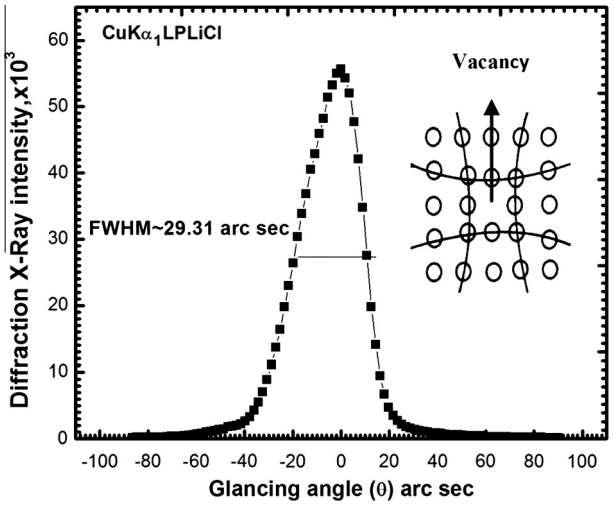

Figure 3 Diffraction curve recorded for a typical LPLCM single crystal using (−2 1 1) diffracting planes with Cu $K\alpha_1$ radiation. Inset shows the schematic of an interstitial defect.

diffuse X-ray scattering) intensity at slightly lower Bragg angles (θ_B) as d and $\sin\theta_B$ are inversely proportional to each other in the Bragg equation ($2d \sin\theta_B = n\lambda$; n and λ being the order of reflection and wavelength respectively which are fixed). The inset in the curve shows the schematic to illustrate how the lattice around the defect core undergoes tensile stress. The converse explanation is true in case of interstitial defects which cause compressive stress in the lattice around the defect core leading to decrease of lattice spacing and in turn results in more scattered intensity at the higher Bragg angles. It may be mentioned here that the variation in lattice parameter is confined very close to the defect core which gives only the scattered intensity close to the Bragg peak. Long range order could not be expected and hence change in the lattice parameter is also not expected (Bhagavannarayana et al., 2010). It may be worth to mention here that the defects are more or less statistically distributed in the crystal. If the defects are not

Please cite this article in press as: Thukral, K. et al., Comprehensive study on L-Proline Lithium Chloride Monohydrate single crystal: A semiorganic material for non linear optical applications. Arabian Journal of Chemistry (2015), http://dx.doi.org/10.1016/j.arabjc.2015.08.022

statistically distributed but distributed here and there as macroscopic clusters leading to mosaic, then the strain generated by such clusters is larger leading to cracks and structural grain boundaries which can be seen very clearly in HRXRD curves with additional peak(s) as observed in our recent study on urea-doped crystals in ZTS at various levels of doping (Bhagavannarayana and Kushwaha, 2010). However, in the present experiments the diffraction curve does not contain any additional peak and indicates the absence of clustering of point defects at macroscopic level. The single diffraction peak with reasonably low FWHM indicates that the crystalline perfection is quite good.

3.3. Photoluminescence (PL) and its decay kinetics

The imperfection or defects present within the crystal can be figured out using photoluminescence (PL) technique for which the emission spectrum was registered at a specific excitation wavelength at room temperature (~20 °C). In the current experiment, the PL decay kinetics have also been determined to explain the lifetime of exciton, which is one of the essential parameters for any device fabrication. This complete analysis of the sample was recorded using Edinburg luminescence spectrometer (Model: F900) equipped with microsecond xenon flash lamp as the source of excitation. Fig. 4(a) shows the PL emission spectrum of the sample registered at an excitation wavelength of 307 nm. The emission peak scrutinized at 469 nm suggests that it lies in the blue region in accordance with the electromagnetic spectrum.

The Time-Resolved PL (TRPL) spectroscopy explains the radiative recombination of the material along a particular transition. The efficiency of the recombination varies with respect to the quality of the grown crystal (Vijayan et al., 2014). The decay time was calculated in terms of microseconds. The decay plots are usually multiexponential in nature but in the current case it followed the trend of biexponential behavior that can be expressed as

$$y = A + B_1 e^{-t/\tau_1} + B_2 e^{-t/\tau_2} \quad (1)$$

where τ_1 and τ_2 represent the fast and slow decay components of lifetime, A, B_1 and B_2 are constants, which determine the contributions of the fast and slow decay components. TRPL plot was shown in Fig. 4(b). The fitting of the curve was further performed by splitting the curve in two regions i.e. region I and region II for simplicity and accuracy sake. The decay constants for the regions I and II have been observed to be 2873.062 μs and 1756.7055 μs, respectively.

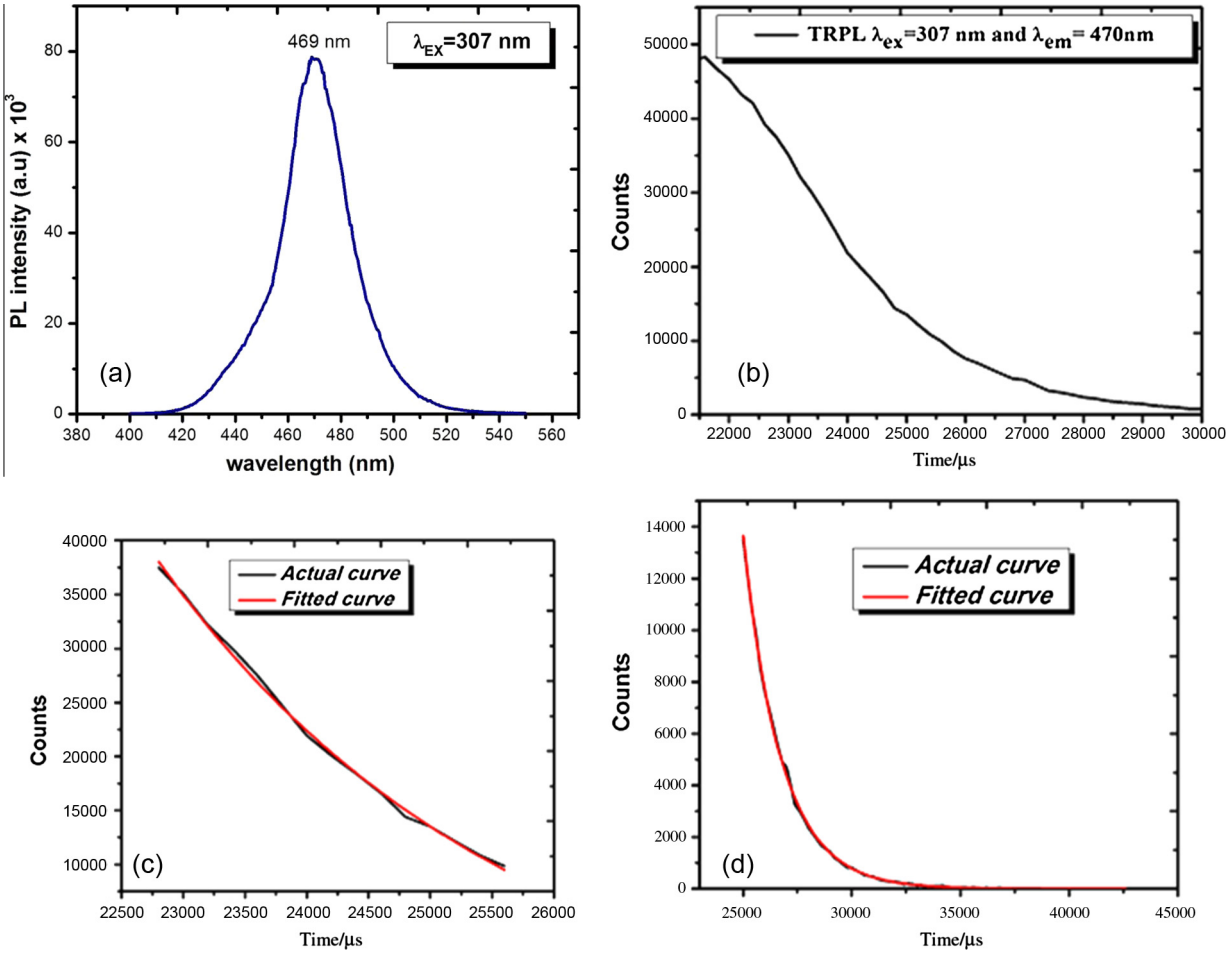

Figure 4 PL spectrum for LPLCM single crystal and (b) Time resolved PL decay on room temperature.

3.4. Birefringence

Birefringence is one of the important optical analyses for nonlinear optical single crystal because it will give an idea about the homogeneity and defects in the grown specimen. In the present study, the modified channel spectrum (MCS) method has been employed for quantitative assessment of the optical quality of the grown specimens. Highly perfect and polished surface of LPLCM crystal have been used for the dispersion of birefringence experiment. When light passes through the LPLCM, the extraordinary and ordinary waves have a wavelength of λ/n_e and λ/n_o respectively, that are perpendicular to each other. The light wave exit from the flat surface of the LPLCM has 180° phase difference between two polarized components. The values of the birefringence have been calculated by finding the absolute fringe order for particular wavelength and computed using the relation: $\Delta n = k\lambda/t$, where λ is the wavelength in nm, t, the thickness of the crystal in mm and k, the fringe order (Bhoopathi et al., 2013). The LPLCM shows two beam interference color fringes in the visible wavelength range of 490–600 nm in Fig. 5(b). The graph drawn between birefringence (∇n) and wavelength (λ) is represented in Fig. 5(a). The birefringence value of the conventional grown crystals was found to be 0.053384 at the wavelength 600 nm for the thickness of 131 μm. It is necessary to have the large value of birefringence i.e. the crystal carries wide range of phase matching angles when a NLO crystal was subjected for harmonic generation or parametric oscillation device. However, the converting efficiency of the laser in harmonic generation is lowered as the birefringence of the crystal becomes larger. Therefore, if the crystal is used only in harmonic generation device with a particular wavelength range, only the minimum birefringence of the crystal which causes phase matching is required. The low birefringence value ($\Delta n = 0.0573$ at $k = 532$ nm) indicates that the crystal is suitable for harmonic generation device (Krishnan et al., 2014). The obtained values were found to be positive integer and decrease with increasing wavelength, which illustrated the grown LPLCM possess negative dispersion of birefringence and crystal belongs optically positive at room temperature respectively. In a case if the crystal carries the negative dispersion then it can be used to balance the positive dispersion of the laser medium (Fork et al., 1984). A slight dispersion shows in birefringence can highly be helpful in frequency conversion processes such as second and other high order harmonics generations (Yariv and Yeh, 1984). The plot Fig. 5(b) depicts some distortions from the linearity curve, which may be due to the short range defects in the specimen and is in tune with HRXRD (FWHM) value. The interference pattern of birefringence is an important tool to determine the optical homogeneity and defects in the crystals (Sangeetha et al., 2011). The dispersion pattern shows non uniform fringes in LPLCM and it suggested signature of slight nonhomogeneity inside the crystal. In the pattern, the fringes are seen with slight disturbance which may be due to the slight defects or thermo dynamical considerations during the growth of LPLCM from solution.

3.5. Dielectric measurements

In case of nonconducting materials, the dielectric measurements are related to the electro-optic properties of the materials. The dielectric measurements have been carried out by using 'Alfa-A' high impedance analyzer (Nova Control technologies). The silver coating has been applied along both sides of plane (−2 1 1) that act as an electrode. Fig. 6a, 6b shows the dielectric constant (ε_r) and dielectric loss ($\tan\delta$) with respect to the frequency over a range of 10 Hz–10 MHz at room temperature. It was observed that the ε_r values are higher at low frequency because of the presence of four types of polarization (i.e. space charge, dipolar, ionic and electronic polarizations) but at 1 kHz frequency its values become constant. The decrement in the values of ε_r at higher frequency is due to contribution of ionic and electronic polarization only (Riscob et al., 2011). As lower the value of the dielectric constant more the material will suitable for the enhancement of SHG property, with respect to Miller rule (Von Hundelshausen, 1971). The behavior of the dielectric loss curve at low frequency was completely depending upon the factors like defects and size of the crystal etc (Przesiawski et al., 1995). The low value of dielectric loss sug-

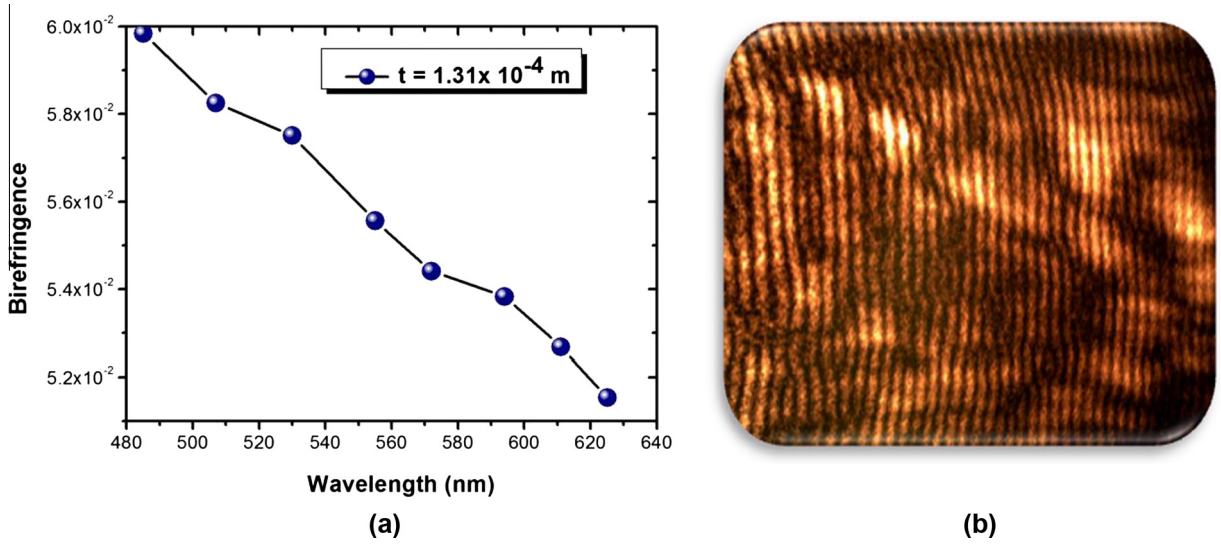

Figure 5 (a) Birefringence interferogram and (b) plot drawn against Birefringence versus wavelength.

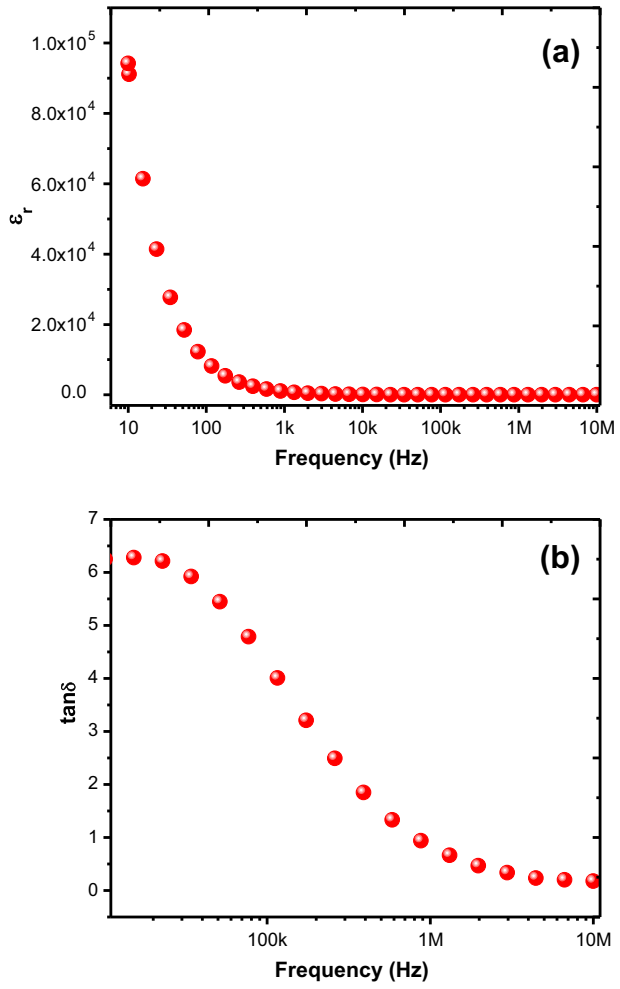

Figure 6 (a) Dielectric constant against frequency and (b) dielectric loss versus frequency.

gests that the crystal has less defects/impurities which were confirmed by HRXRD measurement.

3.6. Laser threshold damage

Before going for any device fabrication it is necessary to analyze the bond strength or thermal stability of the single crystal by applying single shot and multiple shots of laser using laser damage threshold technique. The laser damage threshold of LPLCM was examined by high intensity Nd:YAG laser. In the present study, (−2 1 1) plane was exposed to Nd: YAG laser of wavelength 1024 nm to find out damage cause on surface of the crystal by applying single and multiple shots of the beam (Vanishri et al., 2006). It was seen that if the crystal possesses high specific heat then it carries high resistance toward laser exposure. And at the same time, it generates temperature which causes some damage on the surface of the specimen. Apart from the specific heat, crystalline perfection is also very important reason for laser threshold damage because if the crystal carries high defect density then they get maximum groves of energy absorption and results in the damage of the crystal surface. The values are observed for both single shot and multiple shots and it is given in Table 1. These values are further help in locating the tolerance power of single crystal against laser shots. It was found that the threshold value of multiple shots is less than single shot due to dominance of thermal effect in the single crystal.

Table 1 Damage threshold values on single shot and multiple shots of LPLCM single crystal.

Crystal	Damage threshold			
	at 1 pulse per second		at 10 pulses per second	
	J/cm^2	GW/cm^2	J/cm^2	GW/cm^2
L-Proline Lithium Chloride Monohydrate	5.1	5.1	4.7	4.7

3.7. Z-scan

The variation in the optical absorption properties of a material induced by an intense laser beam can be determined using the open aperture Z-scan technique. In a typical open aperture Z-scan experiment, the laser beam was focused using a Plano-convex lens of focal length 10.75 cm. The laser propagation direction is taken as Z and the sample is scanned along the Z direction through the focal region of the lens in small steps (200 μm) while its optical transmission is being measured. Sample dispersed in distilled water was taken in a1 mm cuvette which was mounted on a stepper motor controlled linear translational stage. The sample experiences different incident intensity (fluence) at each position 'Z' and the corresponding transmission is measured using a pyroelectric energy detector (Rj 735). A frequency doubled output (532 nm) from a Q-switched Nd:YAG laser was used for the Z-scan experiment. The nearly Gaussian laser pulse obtained from the laser has a pulsewidth (FWHM) of 5 ns and the average input laser pulse energy used was 150 μJ (Philip et al., 2012).

The intensity dependent nonlinear transmission measured in the present sample is shown in Fig. 7(a). The sample used has a linear transmittance of 80% at the excitation wavelength of 532 nm. The open aperture Z-scan curve exhibits a valley, which indicates a typical absorptive nonlinearity. The nonlinear transmission as a function of input intensity is plotted in Fig. 7(b). To understand the real mechanism behind this nonlinearity we have numerically fitted the experimental data to deferent nonlinear transmission equation and the obtained nonlinear transmission data are found fit well to a two photon absorption process. From the best fit the nonlinear absorption coefficient is calculated. The nonlinear transmission equation for a third order nonlinear process is given by,

$$T(z) = \left(\frac{1}{\sqrt{\pi} q_0(z,0)}\right) \int_{-\infty}^{+\infty} \ln\left[1 + q_0(z,0)\exp(-t^2)\right] dt \qquad (2)$$

where $T(z)$ is the normalized transmittance, with $q_0(z,0) = \beta I_0(t) L_{eff} \Big/ \left(1 + \left(\frac{z}{z_0}\right)^2\right)$, with β being the two photon absorption coefficient and I_0 the peak on axis intensity. The calculated 2PA coefficient is 1.6×10^{-11} m/W.

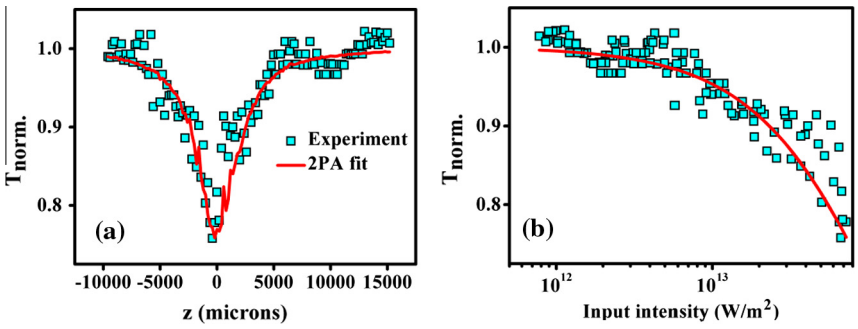

Figure 7 (a) Open aperture Z-scan curve measured for 532 nm, 5 ns laser pulse excitation at an average energy of 150 μJ. (b) Nonlinear transmission as a function of input intensity calculated from the Z-scan curve.

3.8. PPE

Photopyroelectric (PPE) technique is a nondestructive technique which is used to measure the different thermal effects cause due to the periodical variation of temperature of the sample. The main aim of the technique is to determine the thermal parameters such as thermal diffusivity, thermal conductivity, thermal effusivity and specific heat of the crystal at ambient conditions (Menon and Phillip, 2000). The technique is highly beneficial to study the thermal properties of the title compound when it undergoes in phase transitions. Thermal parameters measured using this technique become very helpful when the material undergoes any phase transition such as ferroelectric transition, Para-ferroelectric phase transition and many more.

In the present study, one side of the sample was exposed to the irradiated 120 mW He–Cd laser (λ = 442 nm) and on the other side the temperature variation was recorded by using photopyroelectric detector (Mandelis et al., 1985). The detector was further attached with the thermally thick conductive backing to reduce the temperature fluctuation. The variation in temperature was arisen due to the energy absorption of the crystal which depends on quality of the grown crystal. The pyroelectric detector was 28 μm thick coated with Ni–Cr coated PVDF film, and further the detected PPE signals are amplified and processed with a lock-in-amplifier. For the device fabrication it is necessary to find the exact value of thermal conductivity because if in any case the thermal conductivity find low then it prevents the conduction which results in the accumulation of heat inside the crystal that causes the damage or cracks in the crystal. The phase and amplitude with respect to the frequency has been plotted in Fig. 8. From the curve thermal diffusivity and thermal effusivity were determined. Further these parameters can calculate thermal conductivity and heat capacity by using following relation

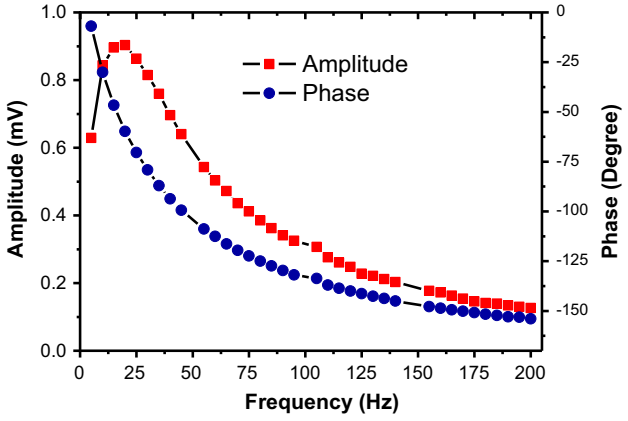

Figure 8 PPE Amplitude Vs Frequency Curve and (b) Phase Vs Frequency Curve for LPLCM single crystal.

$$\lambda_s(t) = e_s(t)\sqrt{\alpha_s(t)} \tag{3}$$

$$C_{ps}(t) = \frac{e_s(t)}{\rho_s(t)\sqrt{\alpha_s(t)}} \tag{4}$$

where λ_s designated as thermal conductivity of sample, e_s is thermal effusivity, α_s is thermal diffusivity and C_{ps} heat capacity at constant pressure of sample. The values of all thermal parameters were enclosed in Table 2.

3.9. Density measurement

The density of LPLCM was calculated experimentally by using floating method. It is the most precise and sensitive way to determine the density of crystal (Vijayan et al., 2006; Andreev and Hartmanoa, 1989). In the present experiment kerosene oil is used as reference. The standard volume of the sinker V_s is 10 cm^3. Initially the density of the kerosene was measured by using following expression

Table 2 Thermal parameters of LPLCM single crystal.

Sample	Thermal diffusivity, α ($\times 10^{-7}$ m^2/s)	Thermal effusivity, e (W m^{-2} K^{-1} $s^{+\sigma}$)	Specific heat capacity, C_p (J/kg K)	Thermal conductivity, K (W/m K)
L-Proline Lithium Chloride Monohydrate	24.09 ± 1.20	769 ± 12	553 ± 8	1.19 ± 0.03

Please cite this article in press as: Thukral, K. et al., Comprehensive study on L-Proline Lithium Chloride Monohydrate single crystal: A semiorganic material for non linear optical applications. Arabian Journal of Chemistry (2015), http://dx.doi.org/10.1016/j.arabjc.2015.08.022

$$\rho_{kero} = \frac{W_{a.s} - W_{k.s}}{V_s} \quad (5)$$

where $W_{a.s}$ is denoted as weight of sinker in air medium, $W_{k.s}$ is weight of the sinker in kerosene medium and ρ_{kero} is density of the kerosene. By using Eq. (5) the density of the crystal can be found out which is clearly expressed in Eq. (6)

$$\rho = \frac{W_a}{W_a - W_k} \times \rho_{kero} \quad (6)$$

where W_a symbolize as weight of sample in air, ρ density of the crystal and W_k weight of sample in kerosene medium. The experimentally measured density value of L-Proline Lithium Chloride Monohydrate is 1.368136 g/cm^3.

4. Conclusions

Slow evaporation solution technique has been adapted to grow L-Proline Lithium Chloride Monohydrate single crystal. The lattice parameters were calculated by single crystal XRD and in addition to this strain present inside the crystal was calculated by powder XRD. Its crystalline perfection was examined by High-Resolution X-ray diffraction which reveals that the sample contains slight point defects and concluded that the crystal quality is optimum for device fabrication. To ensure the HRXRD results photoluminescence has been performed in which the crystal was excited at 307 nm and emission took place at 469 nm i.e. in the visible region. The optical behavior of the single crystal was characterized by using the birefringence. The dielectric constant and dielectric loss have been measured along the particular range of frequency; the lower value of dielectric constant at high frequency gives an excellent sign that the title compound is highly suitable for SHG applications. The two photon absorption coefficient and the thermal parameters were calculated using Z-scan and Photopyroelectric technique respectively.

Acknowledgment

The authors are highly thankful to Director NPL for his constant support and encouragement. One of the authors (K.T) is thankful to UGC (University of Grant Commission) for providing the research fellowship. She is also thankful to Prof. Dr. Reji Philip, RRI, Bangalore, Subhasis Das Dept. of Physics, University of Burdwan, Bardhaman, Dr. B Sridhar, CSIR-IICT, Hyderabad.

References

Andreev, G.A., Hartmanoa, M., 1989. Flotation method of precise density measurements. Phys. Stat. Solid. (a) 116, 457–468.
Balamurugaraj, P., Suresh, S., Koteeswari, P., Mani, P., 2013. Growth, optical, mechanical, dielectric and photoconductivity properties of L-Proline succinate NLO single crystal. J. Mater. Phys. Chem. 1, 4–8.
Batterman, B.W., Cole, H., 1964. Dynamical diffraction of X-rays by perfect crystals. Rev. Mod. Phys. 36, 681–717.
Bhagavannarayana, G., Kushwaha, S.K., 2010. Enhancement of SHG efficiency by urea doping in ZTS single crystals and its correlation with crystalline perfection as revealed by Kurtz powder and high-resolution X-ray diffraction methods. J. Appl. Crystallogr. 43, 154–162.
Bhagavannarayana, G., Parthiban, S., Meenakshisundaram, S., 2008. An interesting correlation between crystalline perfection and second harmonic generation efficiency on KCl-and oxalic acid-doped ADP crystals. Cryst. Growth Des. 8, 446–451.
Bhagavannarayana, G., Kushwaha, S.K., Shakir, M., Maurya, K.K., 2010. Effect of necking on Czochralski-grown LiF crystals and its influence on crystalline perfection and the correlated physical properties. J. Appl. Phys. 44, 122–128.
Bhoopathi, G., Jayaramakrishnan, V., Ravikumar, K., Prasanyaa, T., Karthikeyan, S., 2013. The birefringence spectroscopic studies on ferroelectric glycine phosphite (GPI) single crystals. Mater. Sci. Poland 31, 1–5.
Chemla, D.S., Zyss, J., 1987. In: Nonlinear Optical Properties of Organic Molecule and Crystal, vol. 1 and 2. Academic Press, New York.
Fleck, M., Ghazaryan, V.V., Petrosyan, A.M., 2015. Growth and characterization of L-prolinium phosphate. J. Mol. Struct. 1079, 460–464.
Fork, R.L., Martinez, O.E., Gordon, J.P., 1984. Negative dispersion using pairs of prisms. Opt. Lett. 9, 150–152.
Kalaiselvi, D., Mohan Kumar, R., Jayavel, R., 2008. Crystal growth, thermal and optical studies of semiorganic nonlinear optical material: L-lysine hydrochloride dehydrate. Mater. Res. Bull. 43, 1829–1835.
Krishnan, P., Gayathri, K., Bhagavanarayana, G., Jayaramakrishnan, V., Gunasekaran, S., Anbalagan, G., 2013. Growth, spectral, thermal, dielectric, mechanical, linear and nonlinear optical, birefringence, laser damage threshold studies of semi-organic crystal: dibrucinium sulfate heptahydrate. Spectrochim. Acta Part A Mol. Biomol. Spectrosc. 112, 152–160.
Krishnan, P., Gayathri, K.P., Rajakumar, R., Jayaramakrishnan, V., Gunasekaran, S., Anbalagan, G., 2014. Studies on crystal growth, vibrational, optical, thermal and dielectric properties of new organic nonlinear optical crystal: Bis (2,3-dimethoxy-10-oxostrychnidinium) phthalate nonahydrate single crystal. Spectrochim. Acta Part A Mol. Biomol. Spectrosc. 131, 114–124.
Kushwaha, S.K., Shakir, M., Maurya, K.K., Shah, A.L., Wahab, M. A., Bhagavannarayana, G., 2010. Remarkable enhancement in crystalline perfection, second harmonic generation efficiency, optical transparency and laser damage threshold in KDP crystals by L-threonine doping. J. Appl. Phys. 108, 033506–0033512.
Mandelis, A., Care, F., Chan, K.K., Miranda, L.C.M., 1985. Photopyroelectric detection of phase transitions in solids. Appl. Phys. A 38, 117–122.
Menon, C.P., Phillip, J., 2000. Simultaneous determination of thermal conductivity and heat capacity near solid-state phase transitions by a photopyroelectric technique. Meas. Sci. Technol. 11, 1744–1749.
Philip, R., Chantharasupawong, P., Qian, H., Jin, R., Thomas, J., 2012. Evolution of nonlinear optical properties: from gold atomic clusters to plasmonic nanocrystals. Nano Lett. 12, 4661–4667.
Przesiawski, J., Lglesias, T., Gonzalo, J.A., 1995. Dielectric characterization of the defect concentration in lithium niobate single crystals. Solid State Commun. 96, 195–198.
Riscob, B., Kushwaha, S.K., Shakir, Mohd., Nagarajan, K., Maurya, K.K., Haranath, D., Roy, S.D.D., Bhagavannarayana, G., 2011. Crystalline perfection, optical and dielectric studies on L-histidine nitrate: a nonlinear optical material. Physica B 406, 4440–4446.
Sangeetha, K., Ramesh Babu, R., Bhagavannarayana, G., Ramamurthi, K., 2011. Unidirectional growth and characterization of L-arginine monohydrochloride monohydrate single crystals. Mater. Chem. Phys. 130, 487–492.
Suresh Kumar, M.R., Ravindra, H.J., Jayarama, A., Dharmaprakash, S.M., 2006. Structural characteristics and second harmonic generation in L-threonine crystals. J. Cryst. Growth 286, 451–456.
Thukral, K., Vijayan, N., Rathi, B., Bhagavannaryana, G., Verma, S., Philip, J., Krishna, A., Jeyalakshmy, M.S., Halder, S.K., 2014a. Synthesis and single crystal growth of L-proline cadmium chloride

monohydrate and its characterization for higher order harmonic generation applications. CrystEngComm 16, 2802–2809.

Thukral, K., Vijayan, N., Singh, B., Bdikin, I., Haranath, D., Maurya, K.K., Philip, J., Soumya, H., Sreekanth, P., Bhagavannarayana, G., 2014b. Growth, structural and mechanical analysis of L-proliniumtartrate single crystal: a promising material for nonlinear optical applications. CrystEngComm 16, 9245–9254.

Uma Devi, T., Lawrence, N., Ramesh Babu, R., Ramamurthi, K., 2008. Growth and characterization of L-prolinium picrate single crystal: a promising NLO crystal. J. Cryst. Growth 310, 116–123.

Uma Devi, T., Lawrence, N., Ramesh Babu, R., Selvanayagam, S., Stoeckli-Evans, H., Ramamurthi, k., 2009. Synthesis, crystal growth and characterization of L-Proline Lithium Chloride Monohydrate: a new semiorganic nonlinear optical material. Cryst. Growth Des. 9, 1370–1374.

Vanishri, S., Bhat, H.L., Deepthy, A., Nampoori, V.P.N., Gomes, E. D., Belsley, M., 2006. Laser damage threshold studies on urea L-malic acid: a nonlinear optical crystal. J. Appl. Phys. 99, 083107–083112.

Vijayan, N., Rajasekaran, S., Bhagavannarayana, G., Ramesh Babu, R., Gopalakrishnan, R., Palanichamy, M., Ramasamy, P., 2006. Growth and characterization of nonlinear optical amino acid single crystal: L-alanine. Cryst. Growth Des. 6, 2441–2445.

Vijayan, N., Philip, J., Haranath, D., Rathi, B., Bhagavannarayana, G., Halder, S.K., Roy, N., Jayalakshmy, M.S., Verma, S., 2014. Bulk growth of ninhydrin single crystals by solvent evaporation method and its characterization for SHG and THG applications. Spectrochim. Acta Part A Mol. Biomol. Spectrosc. 122, 309–314.

Von Hundelshausen, U., 1971. Electrooptic effect and dielectric properties of cadmium-mercury-thiocyanate crystals. Phys. Lett. A 34, 405–406.

Yariv, Yeh, P., 1984. Optical Waves in Crystals. Wiley, New York.

Please cite this article in press as: Thukral, K. et al., Comprehensive study on L-Proline Lithium Chloride Monohydrate single crystal: A semiorganic material for non linear optical applications. Arabian Journal of Chemistry (2015), http://dx.doi.org/10.1016/j.arabjc.2015.08.022